

DOI: <https://www.doi.org/%2010.32792/jeps.v14i2.432>

Optimization of Temperature, Defects, and Thickness for High Efficiency of Tin Halide Perovskites

Hussein.A.Rshash¹, Samir M. Abdul Almohsin^{2,*}

1 Department of Physics, College of Education for Pure Science, Thi Qar University, Nasiriyah, Iraq 64001.

2 Department of Physics, College of Education for Pure Science, Thi Qar University, Nasiriyah, Iraq 64001.

*hussinali.phsx@utq.edu.iq

Received 25 /3/2024, Accepted 12 /5/2024, Published 1 /6/2024



This work is licensed under a [Creative Commons Attribution 4.0 International License](https://creativecommons.org/licenses/by/4.0/).

Abstract:

This research focus on , inorganic $ZrS_2/CH_3NH_3SnI_3/CuO$ layers solar cells through SCAPS-1D software program . In this research, Environmentally friendly solar cells having the arrangement $ZrS_2/CH_3NH_3SnI_3/CuO/Au$. This simulation working the absorber layer $CH_3NH_3SnI_3$ and electron transport material ZrS_2 with hole transport material CuO plus electrode back contact is gold. The study included the effect of several factors (thickness for the active layer , energy band gap, defect density, densities of states in the conduction and valence bands, ETL thickness, band gap, HTL thickness, band gap) on the efficiency of the solar cell. in addition, functioning temperature. We discovered key photovoltaic measures including, Fill factor (FF), Short circuit current density (J_{sc}), Open circuit voltage (V_{oc}), power conversion efficacy (η) for solar cell. The suggested solar cell has a power conversion efficiency of 24.48% with $V_{oc} = 1.7459$ V, $J_{sc} = 33.071$ mA/cm², and FF= 42.4%.

Keywords: inorganic Perovskite, $ZrS_2,CuO,CH_3NH_3SnI_3$, Solar Cells, Simulation SCAPS-1D software .

1-Introduction

Worldwide population growth, the acceleration of technical advancements, and the expansion of underprivileged areas have all contributed to an increase in energy demand and utilization. The predicted level of energy usage in 2050 is 30 terawatts (TW). Accordingly, the silicon (Si) basis accounts for around 90% of the current solar cell market. Si-based solar cells have a number of disadvantages, such as high production costs, weather sensitivity, space requirements, stiffness, pollution issues. Now, A big share of energy loads are fulfilled through the use for nevertheless, Fuels Fossil, The incomplete source are future a national of tiredness [1][2].

Thin-film solar cells (TFSCs) are gaining popularity in photovoltaic (PV) technology because of their low manufacturing costs, well-established fabrication techniques, large-scale production, flexibility, and incredibly efficient power conversion to create more affordable, efficient, and environmentally friendly solar cells[3]. (a-Si) and (CdTe), too, (CIGS) they best general TFSCs devices. Presently, Find the important research center on transition metal dichalcogenides (TMD) resources equally gifted semiconductor has conventional great attention to become would-be applicants in its place of traditional resources for several tenders specially solar cell by way of, catalysis, biomedical and photodetector and, batteries [1][4]. Because their exceptional the wide range of TMD energy gap (~1.0–2.5 eV), reasonable transporter carriage material goods, too appealing optical absorption natures. As result, suited for highly efficient single-junction or double-junction tandem solar cells[5]. The ZrS₂-based SC (ZrS₂/CuO) exhibited theoretically PCE of merely 23.8 % by 1 μm thickness absorber layer, By a η of 26.7%, the SC structure including ZrS₂/ZnO / CdS /MoS₂/Cu₂O shown special routine, so prominence the appropriateness of ZS₂ as a very operative absorber film for SCS [4][1]. New educations using ZrS₂ structures for Solar cells CZTs /ZrS₂/ AZO and CZTs /ZrS₂/ ZnO: Al has proved η of 17.6% and 9.72%, correspondingly[6].

Zirconium disulfide (ZrS₂), goes to collection four of TMDCS, is N-type semiconductor the tells A little incongruity web with additional absorber resources as Vander power. ZrS₂ is careful as a great candidate to fabricate optoelectronics mostly photovoltaics then it has extraordinary absorption coefficient and energy band gap the could be simply planned to be in the collection of 1.2–2.2 eV. Furthermore, ZrS₂ has numerous single optical and electronic possessions due to quasi 2D typical. Founded on these stuffs[4][6].

Additional, CuO is a semiconductor has bandgap in the variety of 1.2–1.5 eV, decent thermal and electronic structures and usually used at super-conductors, super capacitors, and solar energy drives. In accumulation, Cu₂O is a Safe material, is a narrow direct optical band gap in the series of 1.9–2.3 eV, so employed on optoelectronic expedients. The grouping of n-ZrS₂ thin flicks with other semiconductors P-type with correct level energy position such as CuO [4].

A broad organic–inorganic series of hybrid metal iodide perovskites with the general formulation AMI₃, where A is the methylammonium (CH₃NH₃⁺) or formamidinium (HC(NH₂)₂⁺) cation and M is Sn (1 and 2) or Pb (3 and 4) are reported. The compounds were synthesized using a range of synthetic techniques, and the thermal stability, optical, and electrical properties of the resulting materials are addressed. It is observed that the preparation process has a significant impact on the chemical and physical characteristics of these materials. Optical absorption measurements indicate that 1–4 behave as direct-gap semiconductors with energy band gaps distributed in the range of 1.25–1.75 eV. The compounds exhibit an intense near-IR photoluminescence (PL) emission in the 700–1000 nm range (1.1–1.7 eV) at room temperature[7]. Perovskite materials are very desirable for solar applications due to their unique qualities, which include a high optical absorption coefficient, large carrier mobility, and extensive carrier diffusion lengths[8]. Perovskite CH₃NH₃SnI₃ the Sn²⁺ metal cation was the first divalent metal to be used as a substitute for Pb²⁺ in perovskite solar cells due to its similar electronic structure. Lead perovskite is the most often used hybrid material, however lead toxicity is a health and environmental concern, to overcome this problem, lead-based perovskite material is replaced with tin-based perovskite material. Tin perovskite solar cells have a lower Voc than lead perovskite solar cells. Tin-based perovskite solar cells benefit from the planar heterojunction architecture. Tin perovskite solar cells are fragile in the environment and are soon harmed by the oxidation process. Due to the oxidation of Sn²⁺ into Sn⁴⁺, the device's efficiency is significantly decreased[9][10].

As a result, it paper suggested a new project of ZrS₂ based SC paying CuO As per Hole transport Layer with the structure ZrS₂/CH₃NH₃SnI₃/CuO/Au. The projected consumes be there designed and inspected by simulation software program

SCAPS-1D has been charity to perfect the hetero-junction solar cells thin film means properties. At the Electronics and Information Systems (EIS) Department at the University of Gent in Belgium. the Solar Cell Capacitance Simulator One-Dimensional (SCAPS-1D) application was developed to model solar cells. The continuity equation and Poissons equation are given for the free electrons and holes in the conduction and valence bands, numerical simulations can be credited to its single blend of accuracy, versatility, operative sociability, open-source nature, and the active provision from its communal of users and developers[6][1][11]. This study travels the use of ZrS₂, As ETL to improve ruse show, reaching η 23.78% with Voc is 1.21 V; Jsc is 33.97 mA/cm², FF 57.83%. Additionally, study of the energy gap changed of perovskite layer (1.25-1.75) eV, where success η of 24.48% per Voc is 1.74 V, J_{sc} is 33.07 mA/cm², FF 42.4%. We investigate keen on the impressions of changing the thickness of the a perovskite layer, ETL, and HTL, together with variable the doping concentration and defect density of the perovskite layer. Next, study effect changed energy band gap for ETL, and HTL and effect of different back contact material plus temperature work. The ultimate objective is to achieve increased efficiency using careful consideration of all parameters.

2- Numerical simulation and properties of materials

In the simulations performed here, SCAPS software has been used. SCAPS is a simulation program that is widely used to simulate solar cells. SCAPS is a one-dimensional program for simulation with seven input layers of semiconductors manufactured by a group of researchers from Ghent University, Belgium (Solar cell power simulator). It is not possible to build a solar cell without stimulatory operation, as time and resources are wasted. It does not only minimize the risk, time, and money but also analyzes the properties of the layers and their function to maximize the efficiency of the solar cell. Device simulation is an effective medium to gain more insight into the principles of job of electronic devices, which help to additional improve their presentation[8]. The following Poisson and continuity equation for holes and electrons are used in SCAPS-1D numerical simulation calculations[12]

$$\frac{d^2}{dx^2} \Psi(x) = \frac{e}{\epsilon_0 \epsilon_r} [p(x) - n(x) + N_D - N_A + \rho_p - \rho_n] \quad (1)$$

$$\frac{dJ_n}{dx} = G - R \quad (2)$$

$$\frac{dJ_p}{dx} = G - R \quad (3)$$

where Ψ , e , ϵ_0 , ϵ_r , p , n , N_D , N_A , ρ_p , ρ_n , J_n , J_p , R , and G are electrostatic potential, charge of electron, vacuum permittivity, relative permittivity, hole density, electron density, donor impurities, acceptor impurities, holes distribution, electrons distribution, current densities of electron, current densities of hole, recombination rate, and generation rate, respectively[2][4][6].

The basic four solar cell parameters, namely, Jsc (short circuit current density), FF (fill factor), Voc, and PCE measure the performance. The main physical and geometrical parameters of the materials employed[13][14].Figure1(a) shows the graphic figure of the heterojunction configuration

ZrS₂/CH₃NH₃SnI₃/CuO/Au in the simulation proses . The Solar Cells involves a CH₃NH₃SnI₃ absorber layer, An N-ZrS₂ layer electron transport (ETL), and P-CuO (Copper (II) oxide) Hole transport layer (HTL). In this design, Au applied as the electrode, starting a well Structured means for energy efficient solar conversation. ZrS₂ charity as ETL layer, is one of the most gifted photovoltaic resources owed it is high absorption coefficient and flexible energy band gap of (1.2 _ 2.2) eV, agreeing for fruitful energy adaptation and device production, ZrS₂used as ETL for to its cost effectiveness, physical and chemical steadiness, and Safe.

The varied energy band gap of ZrS₂ (1.8 eV) show a vital role in the heterojunction construction by allowing important optical quantity. Furthermore, CuO is recycled as HTL, efficiently rising the recombination loss of photogenerated transporters at the spinal advantage. Figure1 (b) shows the energy band gap drawing of the stated solar cell construction. Very simulations is showed at AM 1.5 G light.

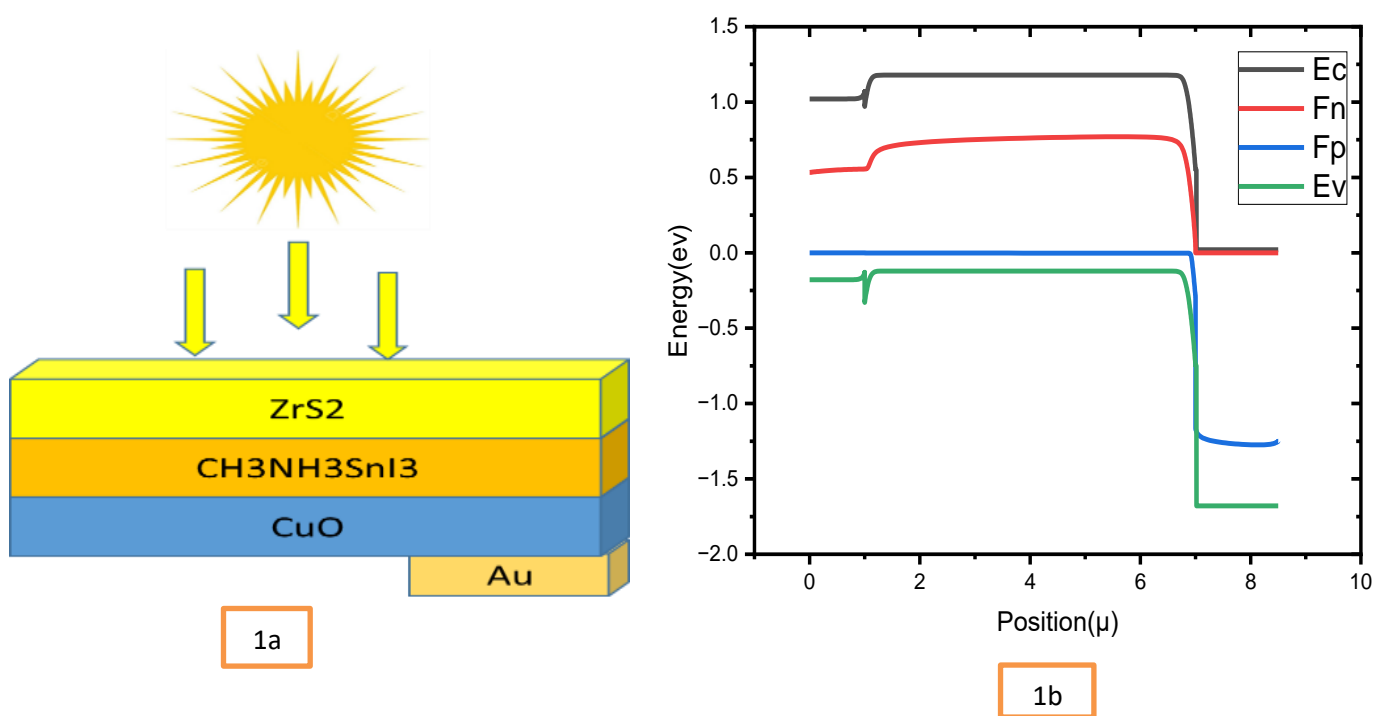


Figure 1.(a) Schematic structure of ZrS₂/CH₃NH₃SnI₃/CuO/Au solar cell (b) energy gaps projects for the materials used.

Factors of changed layers to optimize the performance of the recently developed ZrS₂ ETL CH₃NH₃SnI₃ with Cu₂O HTL. The pertinent physical factors for every layer has been defined at Table1 ⁽¹⁾[4][9][15][16].

Material parameter	n-ZrS ₂	CH ₃ NH ₃ SnI ₃	p-CuO
Thickness	50 nm	9μm	100 nm
Band gap, E _g (eV)	1.8	1.35	1.3
Electron affinity, χ (eV)	4.7	4.17	4.07
Permittivity(Relative), ε _r	16.4	10	18.1
CB density of states, N _C (1/cm ³)	2.2×10 ⁺¹⁹	1×10 ⁺¹⁹	3×10 ⁺¹⁹
VB density of states, N _V (1/cm ³)	1.8×10 ⁺¹⁹	1×10 ⁺¹⁸	1×10 ⁺¹⁹
Mobility(Electron), μ _n (cm ² /Vs)	3×10 ⁺²	2.4×10 ⁺¹	2×10 ⁺²
Mobility(Hole), μ _h (cm ² /Vs)	3×10 ⁺¹	2.4×10 ⁺¹	2×10 ⁺¹
Effective mass of electrons	4.97×10 ⁻¹	0	7.9
Effective mass of Hole	3.18×10 ⁻¹	0	2.4
Acceptor density, N _A (1/cm ³)	0	1×10 ⁺¹⁶	1×10 ⁺¹⁶
Donor density, N _D (1/cm ³)	1×10 ⁺¹⁹	1×10 ⁺¹²	0
Defect type	Neutral	Neutral	Neutral
Energy distribution	Single	Single	Single

3- Result and Discussion

Impact of CuO thickness, band gap on basic parameters of solar cells.

Now this section, we first study outcome of the hole transport thickness layer on the photovoltaic important factors [short circuit current density (J_{sc}), fill factor (FF), open circuit voltage (V_{oc}) and Solar cell efficiency (η)] , Anywhere the thickness was changing(1-10)μm and(100-900)nm.

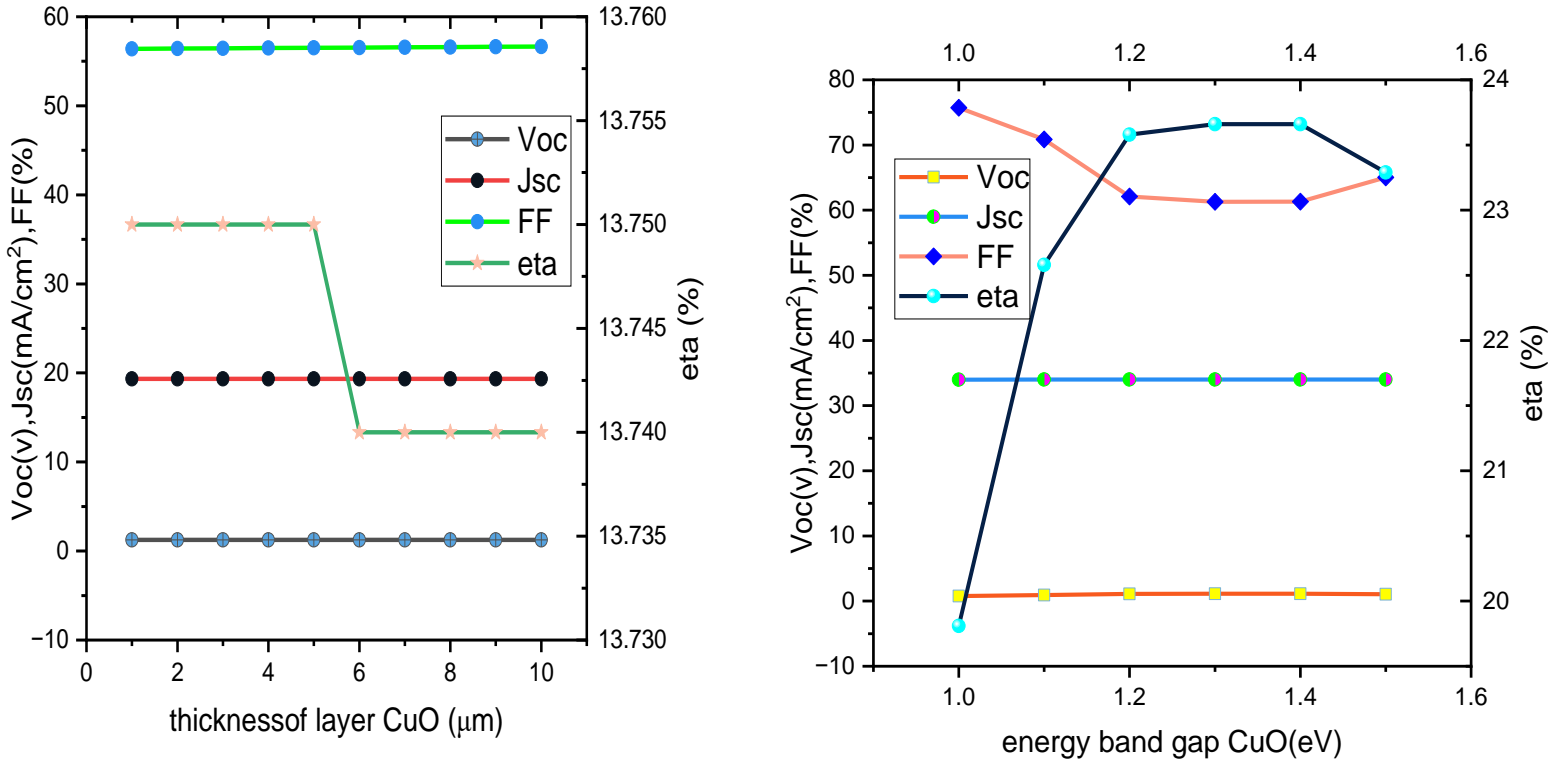
Figure (2) demonstrates the gained line and symbol plot of the showed solar cell basic parameters counting V_{oc}, J_{sc}, FF, and η as the CuO thickness layer from 1μm to10 μm and from 100nm to 900 nm (the x-axis). We notice that there is a slight change in all the basic

Parameters of the solar cell. At thickness (1-10)μm, the V_{oc} decreases from 1.2606v to1.2539v while J_{sc}, FF increase from 19.3391mA/cm² to19.3393mA/cm²,56.40% to 56.66%respectively.for the η drops from

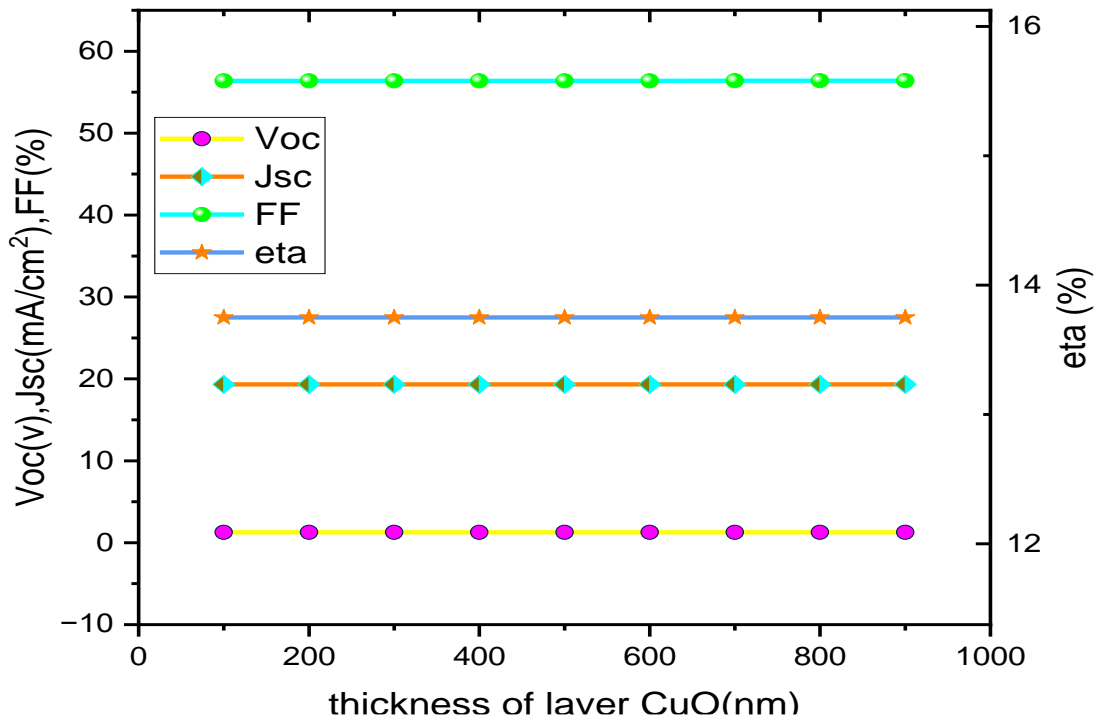
13.75% to 13.74%. As the thickness decreases (900-100)nm, there is a slight variation in the solar cell parameters while the efficiency remains constant at 13.75%. It is obvious that the V_{oc} , the J_{sc} , the FF, and the η have values that remain almost constant with thickness changes of the CuO, which means that the effect of CuO thickness on the basic parameters of solar cells is not noticeable. We notice that the increase in thickness from 1 micrometer to 10 micrometers decreases the efficiency due to reducing the transparent percentage of CuO while the efficiency becomes constant when the thickness of CuO is still transparent and stays at the same value.

Secondly, we study the effect of energy band gap of the hole transport layer on the photovoltaic important factors (V_{oc}), (J_{sc}), (FF), and (η). Everywhere the energy band gap was changing (1-1.5)eV. Figure (3) demonstrates the gained line and symbol plot of the sculpted solar cell basic factors counting V_{oc} , J_{sc} , FF, and η as the energy band gap from 1eV to 1.5eV at (the x-axis). We notice that there is V_{oc} rise from 0.76 volt at 1 eV to 1.13 volt at 1.3 eV and 1.4 eV and drop to 1.05 volt at 1.5 eV while J_{sc} stands at 34 mA/cm², but FF decreases from 75.73% at 1eV to 61.27% at 1.3eV then it rises again to 65.03% at 1.5eV. Finally, Power conversion efficiency enhances from 19.81% at 1eV to 23.66% at (1.3- 1.4) eV, thus drops to 23.29% at 1.5eV.

Those results might be explained equally by energy band gap widening, a confined collection efficiency of bright absorption rise, and the border in CuO too enhances the carrier generation rate [4]. We chose the optimum thickness 100nm and energy gap 1.3eV for CuO.



Figure(2):The variation of $V_{oc}(v), J_{sc}(mA/cm^2), FF(\%), \eta(\%)$ with thickness layer of CuO in(μm) and (nm).



Figure(3):The variation of $V_{oc}(v), J_{sc}(mA/cm^2), FF(\%), \eta(\%)$ with energy band gap for CuO.

Effect of ETL (ZrS₂) thickness, energy bandgap on basic parameters of solar cells.

Figure (4,5) illustrated the impact of ZrS₂ thickness, energy band gap on PV parameters.

We firstly study effect of the electron transport thickness layer on the photovoltaic important factors (V_{oc}), (J_{sc}), (FF), and (η), the thickness was changing(1-10)μm and(50-900)nm.

Figure (4) demonstrates the gained line and symbol plot of the sculpted solar cell basic factors with V_{oc}, J_{sc}, FF, and η as the ZrS₂ layer thickness from 1μm to 10 μm and from 900nm to 50 nm (the x-axis). We notice that there is a difference in all the basic parameters of the solar cell. At thickness(1μm-10μm) the V_{oc}, J_{sc}, η decreases from 1.26v to 1.13v and 19.33 mA/cm² to 13.66 mA/cm² and 13.75% to 9.52% respectively. While FF increase from 56.39% to 61.15%. conversely, at thickness(900nm-50nm) the J_{sc}, η increase from 19.88 mA/cm² to 33.97 mA/cm² and 14.15% to 23.78% respectively. As for V_{oc}, FF decreases 1.26 volt to 1.21 volt and 56.13% to 55.54% thus it rises again to 57.83% respectively.

It could be explained that the amount of light that inter through the window (ZrS₂) will reduce as a result to increase the thickness of materials so the photocurrent drop and saturation current. Therefore, efficiency decreases as thickness increases.

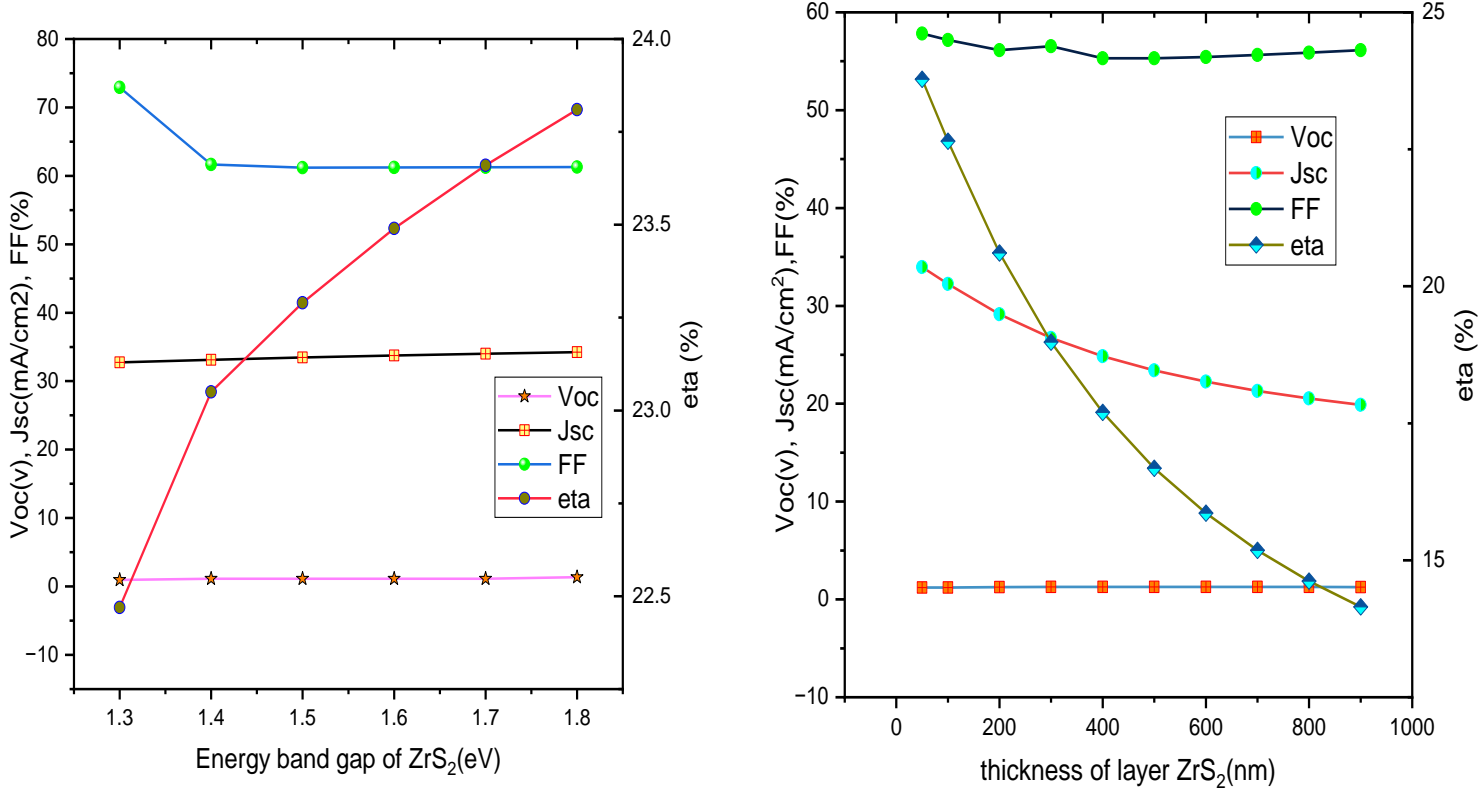
Secondly, we study effect energy band gap of the electron transport layer on the photovoltaic important factors (V_{oc}), (J_{sc}), (FF), and (η). the Energy Band gap was changing (1.3-1.8)ev.

Figure (5) demonstrates the gained line and symbol plot of the sculpted solar cell basic factors plus V_{oc}, J_{sc}, FF, and η as the energy band gap from 1.3ev to 1.8ev at (the x-axis). We notice that there is V_{oc}, J_{sc} and η increased from 0.94 volt to 1.34 volt, and 32.75mA/cm² to 34.23mA/cm², also from 22.47% to 23.81% respectively. While FF decreases from 72.92% to 61.30%. by increasing the ZrS₂ energy band gap together the V_{oc} and the J_{sc} values reduce and this could be official to augment of recombination process in addition to the leakage current specially per Fixed of ZrS₂ for thickness at 50nm. According to the following equation[4][12][17]

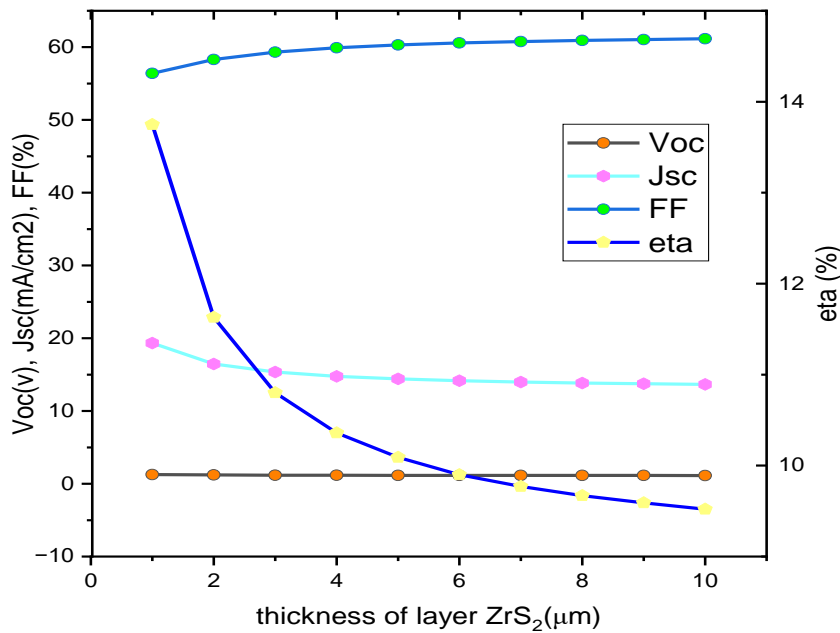
$$\eta = \frac{FFV_{oc}J_{sc}}{P_{in}} \quad (4)$$

$$FF = \frac{V_m J_{mp}}{V_{oc} J_{sc}} \quad (5)$$

Our solar cell optimum ZrS₂ layer thickness was 50nm and band gap 1.8ev for the above results.



figure(4):The variation of $V_{oc}(v)$, $J_{sc}(mA/cm^2)$, $FF(\%)$, $\eta(\%)$ with thickness layer of ZrS_2 in (μm) and (nm).



Figure(5):The variation of $V_{oc}(v)$, $J_{sc}(mA/cm^2)$, $FF(\%)$, $\eta(\%)$ with energy band gap for ZrS_2 .

Impact of perovskite $\text{CH}_3\text{NH}_3\text{SnI}_3$ thickness, bandgap, plus defect, and CB, VB density of states on basic parameters of solar cells.

Figure (6,7) illustrated the impact of $\text{CH}_3\text{NH}_3\text{SnI}_3$ thickness, energy band gap on PV factors. We firstly study of the perovskite layer thickness on the photovoltaic important factors (V_{oc}), (J_{sc}), (FF), and (η). The thickness was changing (1-10) μm and (5-100) μm .

Figure (6) demonstrates the gained line and symbol plot of the sculpted solar cell basic factors excluding V_{oc} , J_{sc} , FF, and η as the thickness at (the x-axis). It is clear from fig.4a that V_{oc} rises as of nearly 0.84v At thickness 1 μm to about 0.9v at thickness 10 μm ,while the difference of the V_{oc} decreased from about 4.57v at thickness 100 μm to about 1.07v at thickness 5 μm ,the J_{sc} value is rise from about 17.01 mA/cm^2 to 19.35 mA/cm^2 with the increase of the thickness from 1 μm to 10 μm , the J_{sc} value remains almost constant for each $\text{CH}_3\text{NH}_3\text{SnI}_3$ thickness which variation from 100 μm to 5 μm ,the FF value is increase from about from 66.41% at thickness 1 μm to about 79.46% at thickness 10 μm while it rises from 17.19% to 63.22% with the diminution thickness from 100 μm to 5 μm ,the η value is increase from about from 9.60% at thickness 1 μm to about 13.87% at thickness 10 μm while it decrease from 15.38% at thickness 100 μm to 12.99% at thickness 5 μm . When the thickness of the perovskite layer increases the efficiency of the solar cell increases .It indicates increased electrons decreased resistance, thus leading to the accumulation of electrons in perovskite, can see the increase of V_{oc} , J_{sc} and FF with the increase thickness [10][18].

Secondly, the study has been included effect of the $\text{CH}_3\text{NH}_3\text{SnI}_3$ energy band gap on the photovoltaic important factors (V_{oc}), (J_{sc}), (FF), and (η), where the E_g was changing (1.25-1.75) eV.

Figure (7) demonstrates the gained line and symbol plot of the sculpted solar cell basic factors comprising V_{oc} , J_{sc} , FF, and η as the energy band gap from 1.3ev to 1.8ev at(the x-axis). It is clear from fig.4b that V_{oc} increases from about 0.88v at E_g 1.25ev to about 9.77ev at E_g 1.7 ev while the V_{oc} be zero at E_g 1.75ev.The J_{sc} value is decrease from about 35.59 mA/cm^2 to 19.08 mA/cm^2 with the increase of the E_g from 1.25ev to 1.75ev.The FF value is decrease from about from 73.63% at E_g 1.25ev to about 8.04% at E_g 1.7ev while it be zero at E_g 1.75ev.The η value is rise from about 23.15% at E_g 1.25ev to about 24.48% at E_g 1.35ev then decrease from about 24.29% at E_g 1.4ev to about 15% at E_g 1.75ev.

The low energy gaps in tin perovskite solar cells enhance the absorption of sunlight and greater conversion efficiency at an energy gap of 1.35eV. In the case of larger gaps, higher energy photons are needed so that the electrons can move to the conduction band, thus reducing the efficiency of the solar cell.

Figure (8) demonstrate the impact of defect density $\text{CH}_3\text{NH}_3\text{SnI}_3$ on solar performance parameters, J_{sc} , FF, V_{oc} , and η with differences of defect density. At this point, defect density is diverse from 1×10^1 to $1 \times 10^{20} \text{ cm}^{-3}$. V_{oc} remains constant at a value 1.745V then begins to decline at a value $1 \times 10^{12} \text{ cm}^{-3}$ from 1.742V to 0.780V. J_{sc} remains constant at a value 33.071 mA/cm^2 then begins to decline at a value $1 \times 10^{12} \text{ cm}^{-3}$ from 33.699 mA/cm^2 to 5.798 mA/cm^2 . The fill factor remains constant at a value 42.4% then begins to increase at a value $1 \times 10^{11} \text{ cm}^{-3}$ from 42.41% to 62.89% at 1×10^{16} then decay to about 55.91% to about 37.75% then rise to 42.79%. Efficiency remains constant at a value 24.48% then begins to decline at a value $1 \times 10^{12} \text{ cm}^{-3}$ from 24.47% to 1.94%. It is clear that increasing the defect density more than $1 \times 10^{12} \text{ cm}^{-3}$ for the perovskite layer leads to reducing the conversion efficiency of the solar cell. This is because the defect density locations are as recombination centers which reduces the numbers Photogene rated carriers. It means defect density decreased by the perovskite layer's crystallinity it causes perovskite solar cells to operate more efficiently [8].

Finally, we were studied impact of conduction band (CB) and valence band (VB) densities of states. Figure (9) shows the impact of conduction band (CB) and valence band (VB) densities of states on solar performance parameters. For CB density variation, VB density is fixed at $1 \times 10^{12} \text{ cm}^{-3}$. Here; CB density varies from 1×10^{12} to $1 \times 10^{21} \text{ cm}^{-3}$. The V_{oc} remains constant at a value 2.51V then begins to decline at a value $1 \times 10^{18} \text{ cm}^{-3}$ from 2.49V to 0.88V at $1 \times 10^{21} \text{ cm}^{-3}$. The J_{sc} fixed at 30.24 mA/cm^2 with CB density variation. The FF remains constant at a value 30.28% then begins to rise from 30.29% to 78.81%. The η remains constant at a value 23.04% then decline from 23.03% to 21%. An increase in the conduction band density of states in perovskite-based solar cells can lead to higher recombination rates and reduced open-circuit voltage, thereby decreasing the overall efficiency of the solar cells.

Figure (10) demonstrates the solar cell output parameters V_{oc} , J_{sc} , FF, and η with variations of Valence Band (VB) density. Here, VB density is varied from 1×10^{12} to $1 \times 10^{21} \text{ cm}^{-3}$, CB density is fixed at $1 \times 10^{12} \text{ cm}^{-3}$. Here, VB density varies from 1×10^{12} to $1 \times 10^{21} \text{ cm}^{-3}$. The V_{oc} is fixed at 2.51v then decreased from 2.49V at a value $1 \times 10^{15} \text{ cm}^{-3}$ to 0.89V at $1 \times 10^{21} \text{ cm}^{-3}$. The J_{sc} is fixed at 30.24 mA/cm^2 then increases from 30.28 mA/cm^2 at a value $1 \times 10^{15} \text{ cm}^{-3}$ to 34.32 mA/cm^2 at $1 \times 10^{21} \text{ cm}^{-3}$. The FF increased from 30.28% to 59.95%. The η remains constant at a value 23.04% then increase to 23.79% then decreased to 18.49%. An initial rise in valence band density enhances hole transport, boosting solar cell efficiency. However, excessive increases lead to detrimental effects like heightened recombination and energy misalignment, causing efficiency to decline. Achieving optimal solar cell performance in perovskite materials demands a delicate balance in tuning electronic properties.

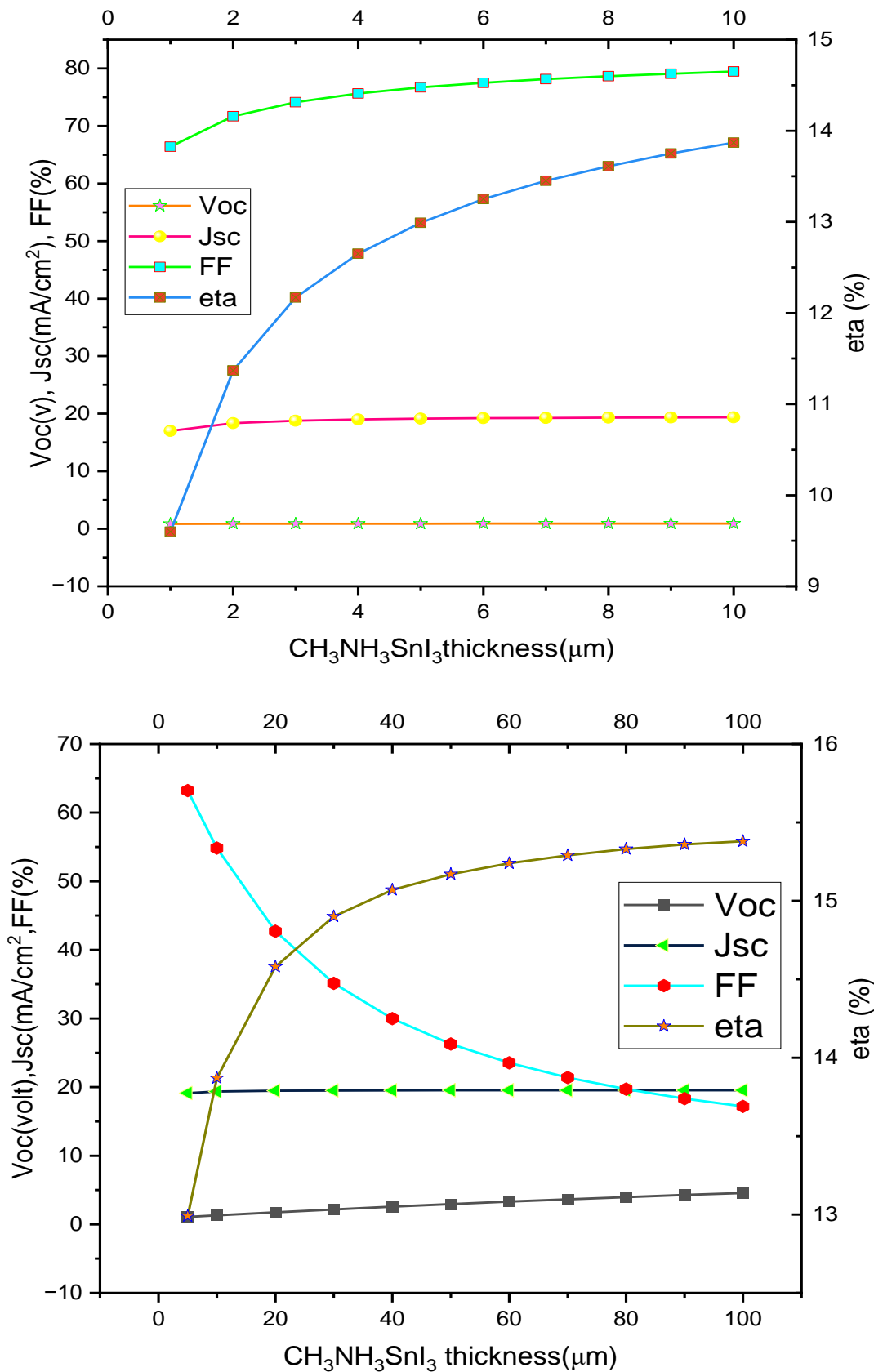


Fig.(6): The variation of $V_{oc}(v)$, $J_{sc}(mA/cm^2)$, $FF(\%)$, $\eta(\%)$ with thickness layer of $CH_3NH_3SnI_3$ from (1-10) μm and (5-100) μm .

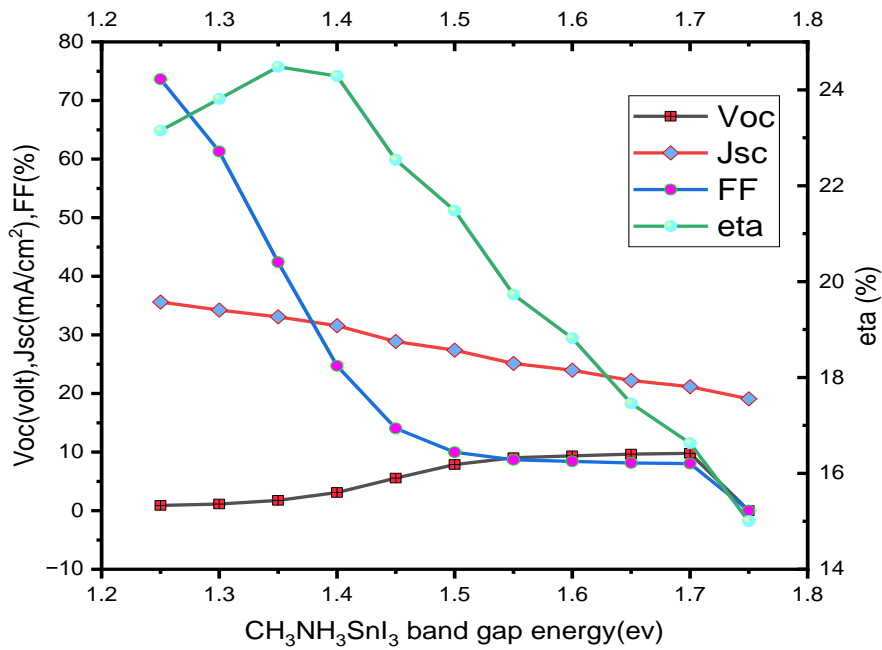


Fig. (7): The variation of $V_{oc}(v)$, $J_{sc}(mA/cm^2)$, $FF(\%)$, $\eta(\%)$ with energy band gap for $CH_3NH_3SnI_3$.

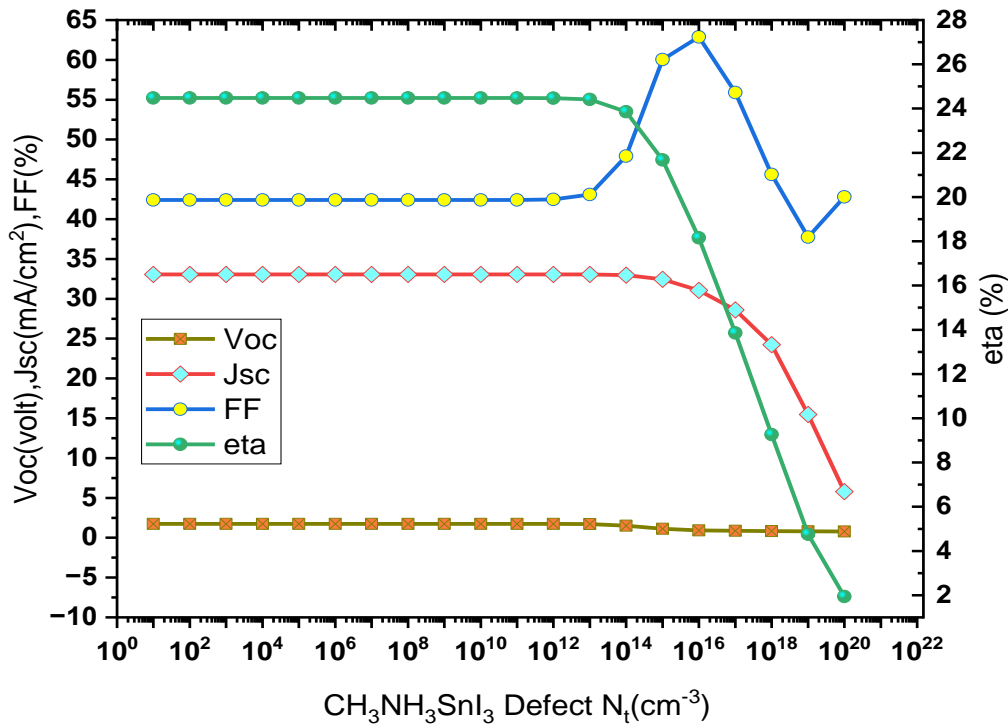


fig.(8): The variation of $V_{oc}(v)$, $J_{sc}(mA/cm^2)$, $FF(\%)$, $\eta(\%)$ with defect N_t for $CH_3NH_3SnI_3$.

9

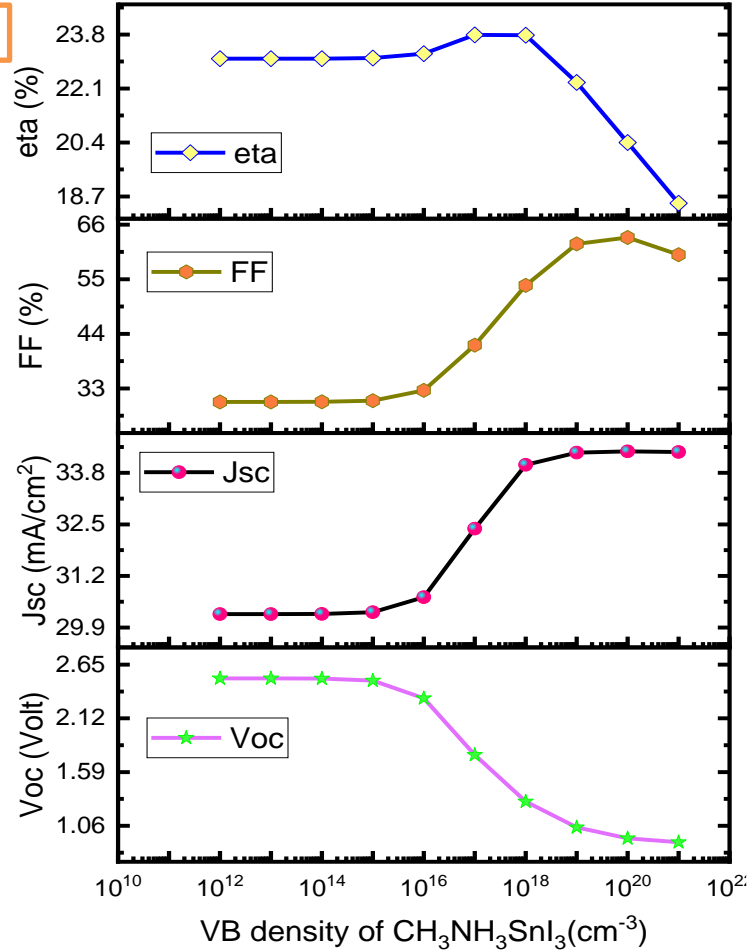
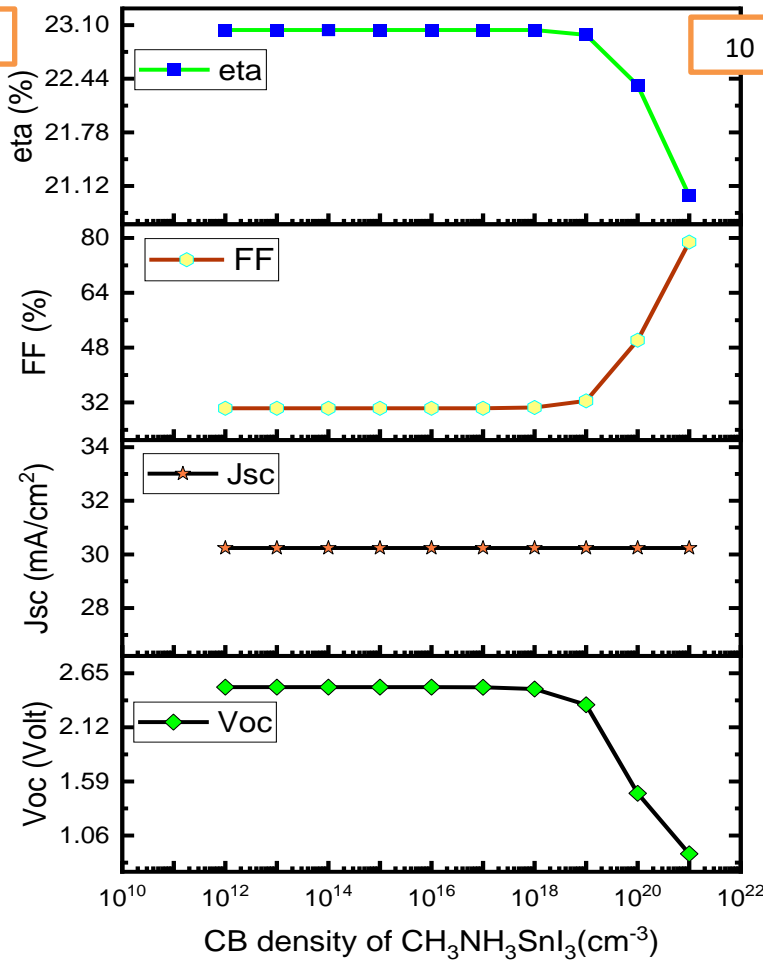


Fig. (9, 10): The variation of V_{oc} (v), J_{sc} (mA/cm^2), FF(%), η (%) with conduction Band (CB) and Valence Band (VB) densities of states of $\text{CH}_3\text{NH}_3\text{SnI}_3$ respectively.

Impact of different back contact material on performance parameters of solar cells.

Figure (11) illustrated the impact of different back contact material on performance parameters of solar cells. The back contact must be manufactured of an acceptable work function material. Variation of the back contact work function (Back) from (4.5 - 5.2) eV was used to get an acceptable back contact for simulation. The increase can be observed The metal work function value increases the open circuit voltage and power conversion efficiency. This is explained by the fact that the carrier majority barrier The height decreases as the value of the work function increases, leading to the ohmic contact [19]. Table 2 shows effect of various metal contact on the efficiency of the cell. Co, Au, Pt, Ni is the most suitable back contact in solar cell.

Table 2: shows effect of various metal contact on the efficiency of the cell

Back contact Metal	Work Function (ev)	Voc volt	Jsc mA/cm ²	FF %	Eta %
Cr	4.5	0.5701	33.899846	71.35	13.79
Si	4.6	0.6701	33.943269	73.99	16.83
Ag	4.7	0.7697	33.977032	76.10	19.90
Ta	4.8	0.9475	34.001459	70.33	22.66
Zn	4.9	1.1048	34.007222	62.62	23.53
Co	5	1.1160	34.07602	62.12	23.58
Au	5.1	1.1165	34.007653	62.10	23.58
Pt	5.12	1.1165	34.007693	62.10	23.58
Ni	5.2	1.1167	34.009027	62.09	23.58

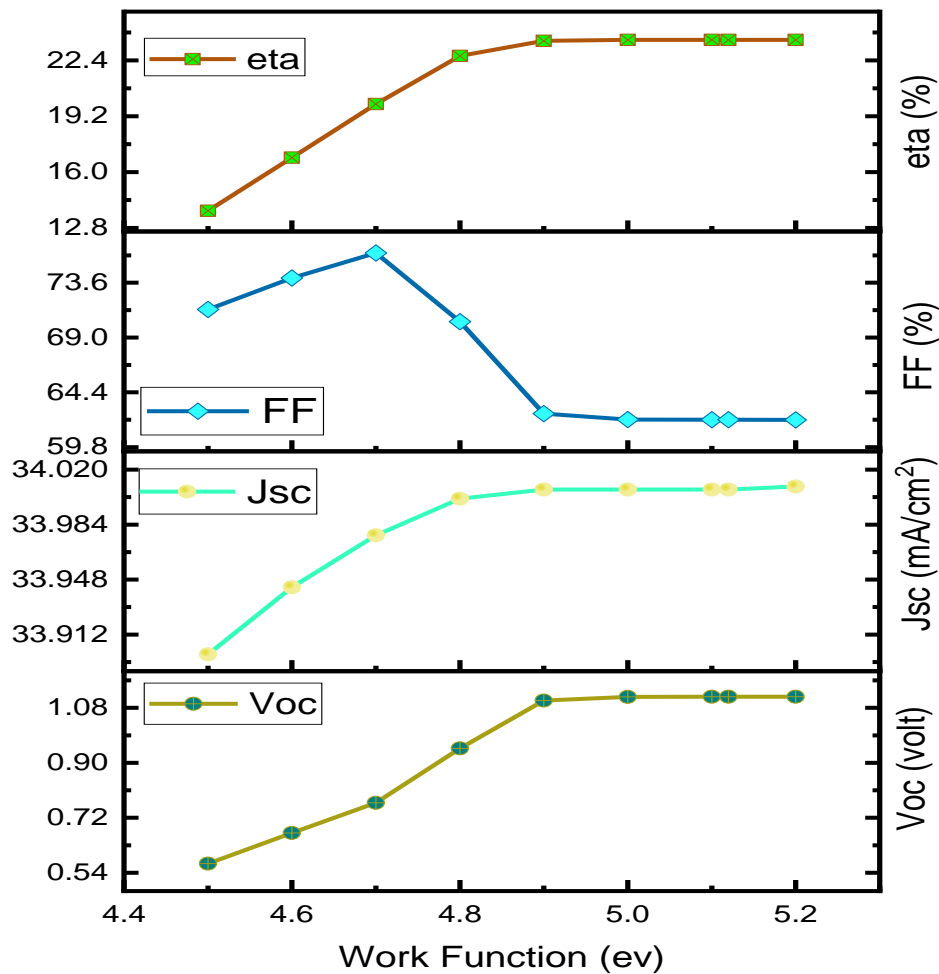


Figure (11) : The variation of $V_{oc}(v)$, $J_{sc}(mA/cm^2)$, $FF(\%)$, $\eta(\%)$ with work function for different back contact.

Effect of Temperature on basic factors of solar cells

The working temperature has important effects on solar cell's efficiency. An operating temperature varies because they are working in various geographical areas with varying seasons and weather. Temperature affects efficiency, as seen in Figure (12) increasing of operation temperature rise the V_{oc} from 1.07v to 1.26v then decreased to 0.94v while the J_{sc} values increased from 32.86mA/cm² to 34.01mA/cm². the FF decrease from 64.66% to 56.86% then rise to 71.78% .for the η increased from 22.94% to 23.62% then dropped to 23.04% with rising temperature from 213 to 333 K. As shown in the figure (12) effects of different temperature ranges on performance parameters of solar cells. Raising the operating temperature typically leads to a decrease in open-circuit voltage (V_{oc}) because it amplifies the reverse saturation current, causing V_{oc} to drop. On the other hand, short-circuit current (J_{sc}) slightly improves as temperatures climb, due to enhanced electron-hole pair production. In the proposed model, the fill factor

(FF) exhibits a non-linear trend, decreasing initially and then increasing as temperatures rise. whereas the temperature increases, the cell efficiency increases to a certain extent and then decreases. due to enhanced charge carrier mobility and generation. However, beyond a certain temperature, efficiency declines because of increased recombination rates and thermal degradation of the perovskite material[1].

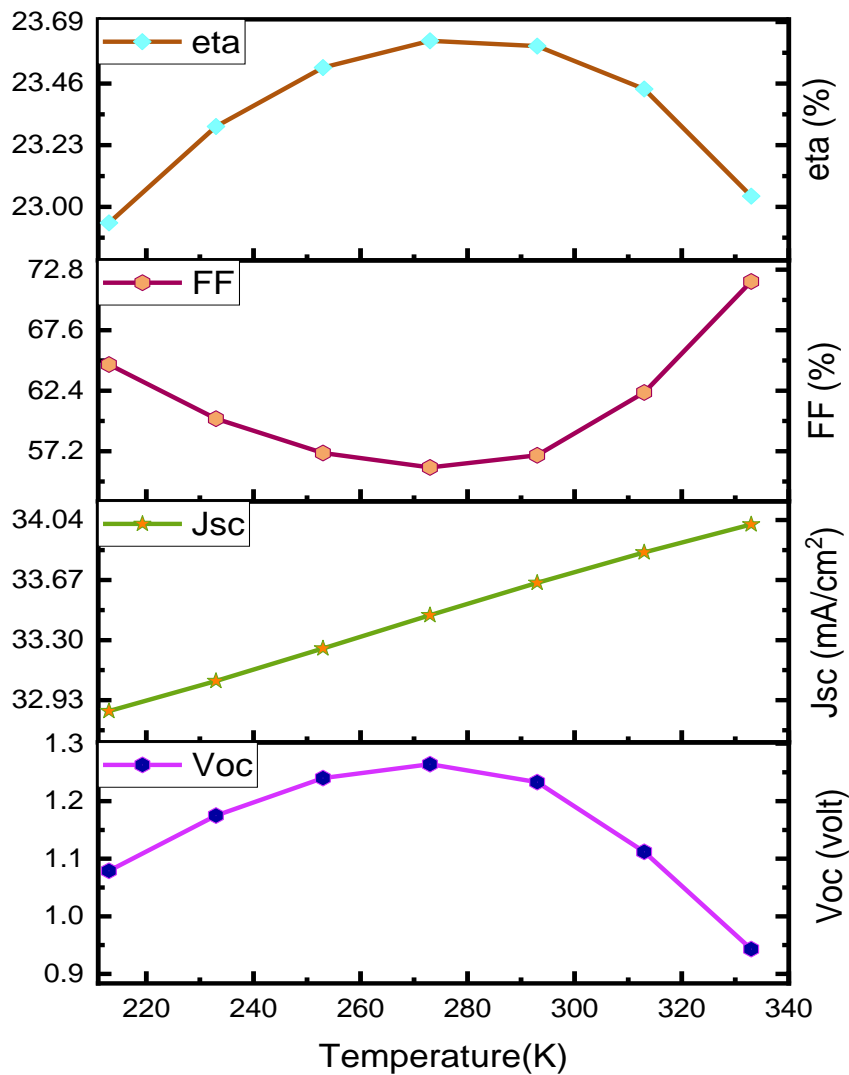


Figure (12): The variation of $V_{oc}(v)$, $J_{sc}(mA/cm^2)$, $FF(\%)$, $\eta(\%)$ with different temperature.

4-Conclusion

This study represents the configuration of structure (Au/CuO/CH₃NH₃SnI₃/ZrS₂) by simulation when SCAPS-1D. When the difference absorber layer used band gap, thickness, defect density, densities of states in the conduction and valence bands. and for the electron transport layer also hole transport layer CuO. Next different electrodes as material Cr, Si, Ag, Ta, Zn, Co, Au, Pt, Ni. In addition, operating temperature is varied from 213 K to 333 K.

The result of our simulation for active material CH₃NH₃SnI₃ are that the optimum thickness, defect density, band gap, CB, VB densities of study are 9 μm, $1 \times 10^{11} \text{ cm}^{-3}$, 1.35 eV, 1×10^{19} , 1×10^{18} respectively. In addition, we find the optimum conditions for ZrS₂ layer when to be 50 nm, 1.7 eV. Finally, optimum conditions for CuO layer when to be 100 nm, 1.3 eV. The back contact electrode as gold to be best metal corresponding to the higher efficiency solar cell 24.48% with V_{oc} 1.7459 V, J_{sc} 33.071 mA/cm², and FF 42.4%.

The study tells that CH₃NH₃SnI₃ absorber layer and ETL (ZrS₂) and HEL CuO are potential goods for photovoltaic used.

REFERENCES

- [1] M. F. Wahid, U. Das, B. K. Paul, S. Paul, M. N. Howlader, and M. S. Rahman, "Numerical Simulation for Enhancing Performance of MoS₂ Hetero-Junction Solar Cell Employing Cu₂O as Hole Transport Layer," *Mater. Sci. Appl.*, vol. 14, no. 09, pp. 458–472, 2023, doi: 10.4236/msa.2023.149030.
- [2] N. S. N. M. Alias, F. Arith, A. N. Mustafa, M. M. Ismail, N. F. Azmi, and M. S. Saidon, "Impact of Al on ZnO Electron Transport Layer in Perovskite Solar Cells," *J. Eng. Technol. Sci.*, vol. 54, no. 4, 2022, doi: 10.5614/j.eng.technol.sci.2022.54.4.9.
- [3] and A. Z. M. T. I. Md. Hasan Ali,* Md Abdullah Al Mamun, Md. Dulal Haque, Md. Ferdous Rahman,* M. Khalid Hossain, "Performance Enhancement of an MoS₂-Based Heterojunction Solar Cell with an In₂Te₅ Surface Field: A Numerical Simulation Approach," *ACS Omega*, vol. 8, pp. 7017–7029, 2023.
- [4] M. Abdelfatah, A. M. El Sayed, W. Ismail, S. Ulrich, V. Sittinger, and A. El-Shaer, "SCAPS simulation of novel inorganic ZrS₂/CuO heterojunction solar cells," *Sci. Rep.*, vol. 13, no. 1, pp.

- 1–14, 2023, doi: 10.1038/s41598-023-31553-4.
- [5] K. Nassiri Nazif *et al.*, “High-specific-power flexible transition metal dichalcogenide solar cells,” *Nat. Commun.*, vol. 12, no. 1, pp. 1–10, 2021, doi: 10.1038/s41467-021-27195-7.
- [6] S. K. Biswas, M. K. Mim, and M. M. Ahmed, “Design and Simulation of an Environment-Friendly ZrS₂/CuInS₂Thin Film Solar Cell Using SCAPS 1D Software,” *Hindawi Adv. Mater. Sci. Eng.*, no. 16878442, p. 10, 2023, doi: 10.1155/2023/8845555.
- [7] and M. G. K. Constantinos C. Stoumpos, Christos D. Malliakas, “Semiconducting Tin and Lead Iodide Perovskites with Organic Cations: Phase Transitions, High Mobilities, and Near-Infrared Photoluminescent Properties,” *Inorg. Chem.*, vol. 52, no. 15, pp. 8285–9162, 2013, [Online]. Available: <https://pubs.acs.org/doi/10.1021/ic401215x>
- [8] M. Kaifi and S. K. Gupta, “Simulation of Perovskite based Solar Cell and Photodetector using SCAPS Software,” *Int. J. Eng. Res. Technol.*, vol. 12, no. 10, pp. 1778–1786, 2019.
- [9] D. I. Tarek, “Study of Hybrid Perovskite Quantum Dot Solar Cells,” 2015.
- [10] D. E. Tareq, S. M. Abdulmohsin, and H. H. Waried, “Perovskite solar cells based on CH₃NH₃SnI₃Structure,” *IOP Conf. Ser. Mater. Sci. Eng.*, vol. 928, no. 7, 2020, doi: 10.1088/1757-899X/928/7/072148.
- [11] A. Slami, M. Bouchaour, and L. Merad, “Numerical Study of Based Perovskite Solar Cells by SCAPS-1D,” *Int. J. Energy Environ.*, vol. 13, pp. 17–21, 2019.
- [12] M. Abdelfatah, W. Ismail, N. M. El-Shafai, and A. El-Shaer, “Effect of thickness, bandgap, and carrier concentration on the basic parameters of Cu₂O nanostructures photovoltaics: numerical simulation study,” *Mater. Technol.*, pp. 1–9, 2020, doi: 10.1080/10667857.2020.1793092.
- [13] G. T. Sayah, “A comprehensive simulation study of methylammonium-free perovskite solar cells,” *Results Opt.*, vol. 11, no. January, p. 100390, 2023, doi: 10.1016/j.rio.2023.100390.
- [14] Zainab. R. Abdulsada and Samir M . AbdulMohsin, “High Efficiency Solar Cells Base on Organic-inorganic Perovskites Materials,” *Univ. Thi-Qar J. Sci.*, vol. 8, no. 2, pp. 23–29, 2021, doi: 10.32792/utq/utjsci.v8i2.808.
- [15] “CuO | PVEducation.” [Online]. Available: <https://www.pveducation.org/pvcdrom/materials/cuo>
- [16] Q. Song, X. Liu, X. Wang, Y. Ni, and H. Wang, “Strain-Tuned Structural , Mechanical and Electronic Properties of Two-Dimensional Transition Metal Sul des ZrS₂ : A First Principles Study1,” *Res. Sq.*, pp. 1–19, 2021.
- [17] M. Moradbeigi and M. Razaghi, “Investigation of optical and electrical properties of novel 4T all perovskite tandem solar cell,” *Sci. Rep.*, vol. 12, no. 1, pp. 1–14, 2022, doi: 10.1038/s41598-022-10513-4.

- [18] A. Luque and S. Hegedus, *Handbook of Photovoltaic Science and Engineering, Second Edition*, book. 2011. doi: 10.1002/9780470974704.
- [19] G. A. Nowsherwan *et al.*, “Numerical optimization and performance evaluation of ZnPC:PC70BM based dye-sensitized solar cell,” *Sci. Rep.*, vol. 13, no. 1, pp. 1–16, 2023, doi: 10.1038/s41598-023-37486-2.